Measurement of Autophagic Activity in Mammalian Cells

Fiona M. Menzies,[1] Kevin Moreau,[1] Claudia Puri,[1] Maurizio Renna,[1] and David C. Rubinsztein[1]

[1]Cambridge Institute for Medical Research, Cambridge, United Kingdom

ABSTRACT

Macroautophagy (referred to herein as autophagy) is a process in which cells engulf portions of cytoplasm in double-membrane vesicles called autophagosomes. These autophagosomes can also capture protein oligomers associated with neurodegenerative diseases, infectious agents (like bacteria), and even organelles (like mitochondria). Autophagosomes are transported along microtubules towards the microtubule organizing center of cells, where the lysosomes are clustered. After fusion and content exchange with lysosomes, the autophagosome cargo is degraded by lysosomal hydrolases. This unit describes some of the core autophagy assays that are in common use, including LC3 immunoblotting, light microscopy analyses of different stages of autophagy, electron microscopy, and an assay of autophagy substrate accumulation. Autophagy assays should generally not be performed alone, but should be accompanied by complementary assays to enable robust interpretations. *Curr. Protoc. Cell Biol.* 54:15.16.1-15.16.25. © 2012 by John Wiley & Sons, Inc.

Keywords: autophagy • LC3 • microscopy • electron microscopy • Huntington's disease

INTRODUCTION

This unit describes some key methods for assessing macroautophagy in mammalian cells. Macroautophagy (referred to henceforth as autophagy) is a process in which cells form double-membrane vesicles around portions of cytoplasm. These autophagosomes can engulf portions of cytoplasm including mitochondria, protein oligomers, and infectious agents such as bacteria. Autophagosomes are then transported along microtubules towards the microtubule organizing center of cells, where the lysosomes are clustered. After fusion and content exchange with the lysosomes, the autophagosome cargo is degraded by lysosomal hydrolases.

Autophagosomes originate from precursor structures that may derive from diverse membrane sources, including the endoplasmic reticulum, mitochondria, and plasma membrane. These precursors contain the autophagic protein complex comprised of autophagy proteins Atg5/Atg12 and Atg16. They may be vesicular, then evolve into three-dimensional crescent-shaped structures called phagophores, the stage when they acquire the key autophagy protein Atg8/LC3.

LC3 is processed by Atg4 to form cytoplasmic LC3-I. After it is conjugated to autophagic membrane-associated phosphatidylethanolamine, it becomes LC3-II and migrates faster on an SDS polyacrylamide gel. As LC3-II is more specifically associated with autophagic membranes, the levels of LC3-II and the numbers of LC3- vesicles correlate with autophagosome abundance. However, the number of autophagosomes does not simply reflect autophagic flux (i.e., the rate of autophagosome delivery to lysosomes).

Current Protocols in Cell Biology 15.16.1-15.16.25, March 2012
Published online March 2012 in Wiley Online Library (wileyonlinelibrary.com).
DOI: 10.1002/0471143030.cb1516s54

Because of the lack of any perfectly specific assay for autophagy, this unit presents four different approaches for assessing this process, including LC3-II immunoblotting (Basic Protocol 1), microscopy for assessing LC3 vesicle flux and assaying preautophagosomal structures (Basic Protocol 2), electron microscopy for assessing autophagosomes (Basic Protocol 3), and the use of mutant huntingtin aggregate counting for assessing autophagy substrate levels (Basic Protocol 4). There are a number of different methods that one can use to assess clearance of autophagic substrates, including measurement of endogenous P62 (an autophagy substrate) and long-lived protein clearance assays (reviewed in Klionsky et al., 2008). We have selected this method as an example, as it allows one to test whether the effects of perturbants are autophagy-dependent, and is suitable for siRNA and cDNA overexpression approaches.

NOTE: All cell lines used in these protocols are cultured under standard culture conditions (see Support Protocol).

BASIC PROTOCOL 1

ASSESSMENT OF AUTOPHAGIC FLUX BY MEASURING LC3-II LEVELS IN THE PRESENCE OF BAFILOMYCIN A_1

To determine the role of a potential autophagy modulator, it is essential to measure autophagic flux, which encompasses the complete lifetime of autophagosomes from their formation to fusion with the lysosomes. This protocol presents the use of immunoblotting to measure LC3 levels as a functional reporter for autophagy and discusses some of the limitations of this widely used approach in studies of mammalian autophagy.

In higher eukaryotes, microtubule-associated protein 1 light chain 3 (MAP1-LC3), the mammalian homolog of yeast Atg8, is the only known protein that specifically associates with autophagosomes and autolysosomes (Kabeya et al., 2000). LC3 is cleaved at its C terminus by Atg4 to form cytoplasmic LC3-I. LC3-I is then covalently conjugated to phosphatidylethanolamine to form LC3-II. LC3-II is specifically targeted to the

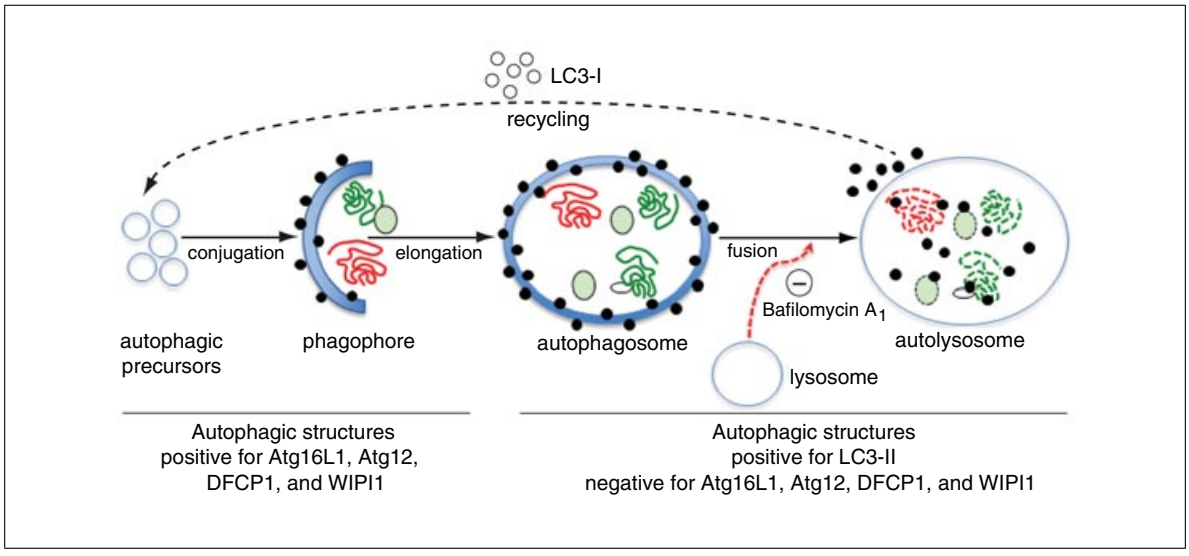

Figure 15.16.1 Localization of autophagic proteins at different steps of autophagosome formation. The cytosolic LC3-I pool (open black circles) is covalently conjugated to phosphatidylethanolamine to form LC3-II (filled black circles). LC3-II localizes to both the cytosolic and lumenal sides of the autophagosome precursor and autophagosome membranes. Ultimately, the outer membrane of the autophagosome fuses with the lysosome, and sequestered components are thereby delivered to the lysosome for degradation by lysosomal enzymes. LC3-II on the lumenal side of the membrane is degraded upon fusion, whereas LC3-II on the cytosolic surface of the membrane can be recycled before or after fusion. Degradation of LC3-II can be prevented with compounds such as bafilomycin A_1 that neutralize the acidic lysosomal pH.

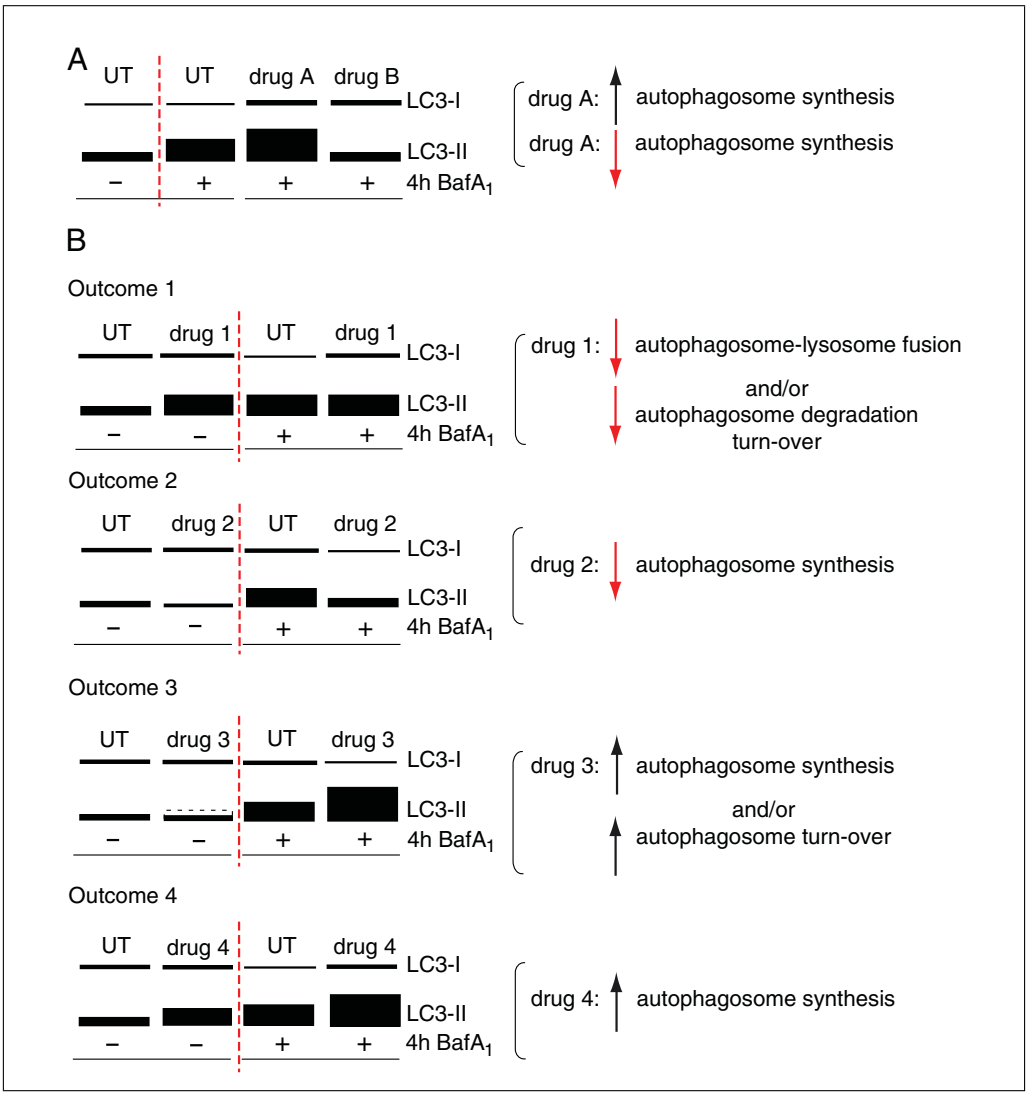

Figure 15.16.2 Measurement of LC3-II levels as a functional reporter of autophagy. Schematic diagrams represent LC3-II immunoblotting results. (**A**) LC3-II levels as a measure of autophagosome synthesis in the presence of an inhibitor of lysosomal proteolysis. The effect of two drugs (A and B) was compared to untreated control cells (UT) in the presence of bafilomycin A1 ($BafA_1$) for 4 hr. (**B**) Theoretical scenarios for measurement of LC3 flux. The effect of a particular compound on autophagosome degradation can be inferred by comparing drug treatment in the absence or presence of inhibitors of lysosomal proteolysis (such as $BafA_1$ used in this example). The four possible outcomes of autophagy modulation by a drug are shown here (drug 1-4). In A and B, levels of loading control (actin or tubulin) are assumed to be constant.

Atg12-Atg5-Atg16 complex at the phagophore and remains associated with the expanding limiting membrane, sealed autophagosomes, and mature autophagosomes/autolysosomes (Fig. 15.16.1). LC3-II is found on both the lumenal and cytosolic surfaces of autophagosomes. The lumenal pool is degraded after fusion with lysosomes, while the LC3-II on the cytosolic side can be delipidated and recycled (Kabeya et al., 2000; Tanida et al., 2004).

During SDS-PAGE, LC3-II migrates faster than LC3-I, allowing the two forms to be distinguished even though both are recognized by anti-LC3 antibodies. Thus, cellular levels of LC3-II (normalized to actin/tubulin loading controls) can be measured as a marker of the number of autophagosomes present in the cell. However, results obtained from immunoblots require careful analysis, as similar changes in LC3-II levels can result from either increased synthesis or decreased degradation. Enhanced autophagosome synthesis

frequently correlates with increased delivery of autophagic substrates to lysosomes for degradation (increased flux). Decreased LC3-II degradation can occur at any point after autophagosome formation, including delayed trafficking to the lysosome, reduced fusion between autophagosomes and lysosomes, or impaired lysosomal proteolytic activity. LC3-II levels will rise over the course of the experiment if the number of molecules generated exceeds the number degraded, even if the *absolute* number of molecules degraded has increased compared to control conditions.

Conversely, decreased levels of LC3-II can be observed if there is a drop in autophagosome synthesis (associated with decreased autophagic flux) or if autophagic flux is induced, which occurs in certain cells under specific conditions (Tanida et al., 2005). Again, LC3-II levels will decrease even if there is an increase in synthesis if the number of molecules generated in the experimental time-frame is less than the number degraded.

To distinguish between different possible interpretations of increased (or decreased) levels of LC3-II, one can measure LC3-II levels under conditions where autophagosome degradation is blocked, i.e., in the presence of lysosomal protease inhibitors (Fig. 15.16.2). Two good candidates are the proton pump inhibitor bafilomycin A_1 and the lysosomotropic chemical ammonium chloride (NH_4Cl), both of which neutralize lysosomal pH (Seglen and Reith, 1976) and block autophagosome-lysosome fusion (Yamamoto et al., 1998). Some investigators have proposed an assay using lysosomal inhibitors (E64 and pepstatin A) to block lysosomal degradation of LC3-II (Tanida et al., 2005). However, E64 may be less than ideal for these purposes, as it is also a calpain inhibitor and calpain inhibition has recently been shown to induce autophagy (Williams et al., 2008). While LC3-II assays are frequently called "autophagic flux" assays, they do not formally assess flux through the autophagic pathway, but rather assess LC3-II synthesis because LC3-II degradation has been blocked (unless the biological system can be shown to be in steady state).

Materials

Cultured cell line (e.g., HeLa cells) or primary culture of interest
Putative autophagy modulator to be tested
Bafilomycin A_1 (see recipe)
Phosphate-buffered saline (PBS, *APPENDIX 2*), ice cold, with and without protease inhibitors (Complete EDTA-free Protease Inhibitor Cocktail tablets, Roche Diagnostics, catalog no. 11 873 580)
Lysis buffer (see recipe)
Protein concentration assay kit (e.g., DC Protein Assay Kit, Bio-Rad)
3× sample loading buffer (see recipe)
Prestained molecular weight marker (e.g., SeeBlue Plus2, Invitrogen)
12% SDS polyacrylamide gel (see recipe)
1× running/transfer buffer (see recipe)
Blocking buffer: 6% (w/v) nonfat dry milk, 0.1% (v/v) Tween-20 in 1× PBS
Primary antibodies: rabbit anti-LC3 (Novus Biologicals), rabbit anti-actin (Sigma-Aldrich)
PBS-T: PBS containing 0.1% (v/v) Tween 20
Secondary antibody: horseradish peroxidise (HRP)−conjugated anti−rabbit IgG (GE Healthcare)
ECL immunoblotting detection reagents (e.g., GE Healthcare)

6-well culture plates
Cell scraper
1.5-ml microcentrifuge tubes
PVDF membrane (Immobilon-P; Millipore)
Extra-thick filter paper (Bio-Rad)

Protein transfer apparatus (e.g., Trans-Blot SD semidry transfer cell, Bio-Rad)
Plastic wrap (e.g., Saran Wrap)
Film cassette (e.g., Hypercassette, GE Healthcare)
High-performance chemiluminescence film (e.g., Hyperfilm ECL, GE Healthcare)
Automated film developer (e.g., RP X-OMAT Processor, Model M6B, Kodak)
Densitometer
Image J software (*http://rsbweb.nih.gov/ij/applet/*)
StatView 4.3 software (Abacus Concepts)

Additional reagents and equipment for SDS-PAGE and immunoblotting (*UNITS 6.1 & 6.2*)

Culture cells to be tested

1. Seed HeLa cells at $2-4 \times 10^5$ per well in 6-well plates. For each putative autophagy modulator to be tested, seed six test wells and six control wells to allow for analysis of LC3-II levels in triplicate wells in the presence and absence of bafilomycin A_1. Culture cells overnight.

   This assay can be performed in various cell lines, such as HeLa, COS-7, SK-N-SH, and mouse embryonic fibroblasts (MEFs), as well as primary cultures, such as human macrophages and mice cortical and striatal neurons. For other cell lines, seed cells at an appropriate density to ensure that there will be sufficient cells to harvest, but that they will not reach complete confluency by the end of the experiment. This will depend on the cell line and must be determined by the investigator.

2. Remove culture medium from the well and replace with medium either with or without the putative autophagy modulator and return to incubator for 24-48 hr.

   The concentration of the compound depends on the experiment. It may be advisable to test various concentrations.

3. During the last 4 hr of treatment, add 400 nM bafilomycin A_1 to the cells in three wells for each treatment condition.

   This approach requires inhibitor concentrations that are saturating for LC3-II accumulation. Furthermore, the lower limit of the duration of bafilomycin A_1 treatment should take into account the half-life of autophagosomes (20-30 min in mammalian cells). In most cases, treating for 4 hr with 400 nM bafilomycin A_1 is sufficient (Fass et al., 2006; Sarkar et al., 2007a,b; Williams et al., 2008). However, doses of inhibitors that are saturating in one cell type are not necessarily saturating in another. Normally, more than a three-fold increase in LC3-II levels can be achieved under these conditions in several routinely used cell lines (Sarkar et al., 2007a,b; Williams et al., 2008) and in primary cultures (Williams et al., 2008; Underwood et al., 2010; Sarkar et al., 2011).

Prepare samples

4. Wash cells three times in enough ice-cold PBS to cover the bottom of the well, then collect the cells into 1 ml of ice-cold PBS containing protease inhibitors using a cell scraper.

5. Transfer cells to 1.5-ml microcentrifuge tubes and centrifuge at $2500 \times g$ at 4°C for 5 min.

6. Discard supernatants and lyse cell pellets with 100-200 µl lysis buffer on ice for 30 min.

7. Centrifuge lysed cells at $6{,}000 \times g$ for 5 min at 4°C to remove cell debris and any unlysed cells. Transfer supernatants to new tubes.

8. Measure protein concentration in each sample (e.g., using a commercially available protein assay kit) and then adjust the volume of the samples so they have equal protein concentrations.

9. Mix 10 μg protein from each sample with 0.5 vol of 3× sample loading buffer (final 1×) and boil at 100°C for 5-7 min in a heating block.

   As an alternative to steps 4-9, cells can be collected by adding Laemmli sample buffer (final 1×) directly to the plate, scraping the cells, and then boiling the samples. This protocol is often more sensitive, allowing small changes in LC3-II levels to be observed; however, it precludes measurement of total protein levels. As equal loading of protein samples is vital for comparison of LC3-II levels in experiments where there may be unequal protein concentrations between samples (e.g., for long-term treatments after seeding), this alternative method is not advisable.

   It is possible for samples to be frozen and stored at −80°C at this stage. However, to optimize sensitivity, freeze-thawing of samples should be avoided, and it is best to perform all required manipulations (from harvesting to SDS-PAGE/transfer) in one working day. Although protein samples can generally be stored at −80°C for a reasonably long time, LC3-II signals appear to be extremely unstable and sensitive to freeze-thaw cycles.

Separate proteins by SDS-PAGE

10. Load protein samples into the wells of a 12% SDS polyacrylamide gel (0.75 or 1.5 mm thick).

    For general information on SDS-PAGE, see UNIT 6.1.

11. Run at 15 mA constant current (per gel) until the marker bands migrate to the desired position.

    As LC3-II migrates at ∼16 kDa, it is important to ensure that a marker of this size does not run too close to the bottom of the gel.

Transfer proteins and perform immunoblotting

12. Cut a PVDF membrane to the size of the gel, activate it by placing in 100% methanol for 30-45 sec, and then equilibrate (along with three extra-thick filter papers) in 1× transfer buffer for 5-10 min. Remove the gel from the glass plates and equilibrate in transfer buffer.

    These steps describe semidry protein transfer; however, samples also may be transferred by wet transfer without any decrease in quality of results. For more information on immunoblotting, see UNIT 6.2.

13. Assemble the gel-transfer unit by placing a filter paper on the base plate of the transfer apparatus, followed by the PVDF membrane, the gel, and finally two more filter papers on top. When placing the gel/filter papers on the membrane, roll the surface gently with a plastic pipet to remove any air bubbles.

14. Complete the assembly by connecting the compression plate and lid, then perform protein transfer at 15 V constant voltage for ∼1 hr.

15. Remove membrane (immunoblot) from the apparatus and incubate in 25 ml blocking buffer with gentle shaking on a rocking platform at room temperature for 1-2 hr.

16. Discard blocking buffer, add primary antibodies diluted in 10-20 ml blocking buffer (anti-LC3 at 1:5000 and anti-actin at 1:3000), and incubate overnight on a rocking platform in a cold room at 4°C.

    Labeling can also be carried out for 1-2 hr at room temperature, but best results are obtained by incubating overnight.

17. Wash immunoblot three times for 10 min each in PBS-T on a rocker at room temperature.

18. Add secondary antibody diluted in blocking buffer (HRP-conjugated anti–rabbit IgG at 1:5000) and incubate for a minimum of 1-2 hr on a rocking platform at room temperature.

19. Wash as in step 17.

20. Combine 1.5 ml each of detection reagents 1 and 2 of the GE Healthcare ECL immunoblotting detection system and add to the immunoblot for 1 min, ensuring coverage of the entire surface.

    For other ECL detection systems, follow manufacturer's instructions.

21. Discard detection solution, wrap the immunoblot in plastic wrap, and place in a film cassette. Expose the blots to film with appropriate exposure times, then develop the film in an automated developer.

    Normally, detection of endogenous LC3-I and LC3-II proteins requires a very short exposure time (5-30 sec on Hyperfilm in a Hyperfilm cassette). The bands for LC3-I and LC3-II appear at 18 and 16 kDa, respectively. Actin is also easily detected with a very short exposure time (usually 10-60 sec) and appears at 45-50 kDa.

Analyze data

22. Perform densitometric analysis of immunoblots from at least three independent experiments using ImageJ software. Set the control condition (without bafilomycin A_1) to 100 and express LC3-II levels (relative to actin) as a percentage, with error bars denoting standard error of the mean. Determine significance levels (p values) by ANOVA factorial test using StatView 4.3.

MONITORING THE NUMBER OF AUTOPHAGOSOMES AND AUTOPHAGIC PRECURSORS BY MICROSCOPY

BASIC PROTOCOL 2

Microscopy-based systems can be used to score the number and size of autophagic precursors and to measure autophagosome turnover, greatly enhancing the autophagic flux analysis.

Autophagosome precursors are characterized by the presence of Atg16L1, Atg12, DFCP1, and WIPI1 among other proteins, whereas autophagosomes are characterized mainly by the presence of LC3 (Fig. 15.16.1; Klionsky et al., 2008; Ravikumar et al., 2010b). Autophagosome formation positively correlates with formation of autophagic precursors, unless a step in the maturation of precursors is blocked, leading to a decrease in the number of fully formed autophagosomes (Ravikumar et al., 2010b; Moreau et al., 2011). The number of autophagic precursors can be monitored by immunostaining for endogenous proteins (Atg12, Atg16L1, and LC3) or by direct imaging of fluorescently tagged exogenous proteins that are either stably expressed (GFP-LC3 in HeLa cells, GFP-DFCP1 in HEK cells) or transiently expressed (GFP-Atg16L1, GFP-LC3).

Autophagic flux can also be analyzed using an mRFP-GFP-HeLa stable cell line (Kimura et al., 2007). This method exploits distinct properties of GFP and RFP. When an autophagosome fuses with a lysosome to form an autolysosome, the low pH inside the lysosome quenches the fluorescent signal of GFP. In contrast, RFP (and other red fluorescent proteins such as mCherry) exhibits more stable fluorescence in acidic compartments (Katayama et al., 2008). By exploiting this difference in the nature of these two fluorescent proteins, autophagic flux can be assessed by examining yellow autophagosomes (i.e., labeled with mRFP and GFP) and red autolysosomes (mRFP only; Fig. 15.16.3). If autophagic flux is increased, both yellow and red punctae are increased; however, if autophagosome maturation into the autolysosomes is blocked, yellow punctae are increased without a concomitant increase in red punctae.

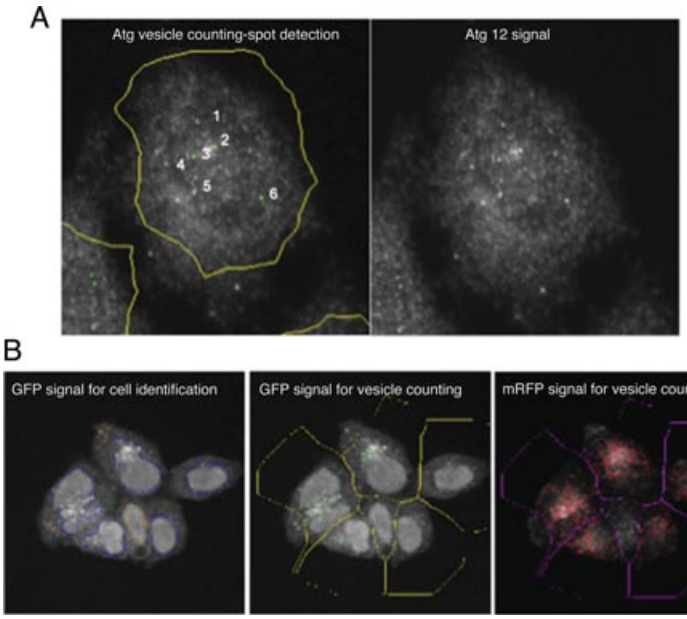

Figure 15.16.3 Automatic counting of Atg12- or LC3-labeled vesicles using a Cellomics ArrayScan VTI HCS Reader. (**A**) HeLa cells were starved for 1 hr, fixed, and immunostained for endogenous Atg12. Left: spot detection for vesicle counting (cell outlines in yellow); right: raw Atg12 signal. (**B**) HeLa cells stably expressing mRFP-GFP-LC3 were fixed and analyzed directly. Left: GFP signal for cell identification; middle, GFP signal for vesicle counting (cell outlines in yellow); right, mRFP signal for vesicle counting (cell outlines in red).

Materials

Cells to be tested: e.g., untransfected HeLa cells, HeLa cells stably expressing GFP-LC3 (Bampton et al., 2005) or mRFP-GFP-LC3 (Kimura et al., 2007), or HEK cells stably expressing GFP-DFCP1 (Axe et al., 2008)

Overexpression plasmid: e.g., GFP-Atg16L1 (Mizushima et al., 2003) or GFP-LC3 (Kabeya et al., 2000)

Transfection reagent (e.g., Lipofectamine 2000, Invitrogen, or TransIT2020; Miras Bio)

Hank's balanced salt solution (HBSS, Sigma)

Phosphate-buffered saline (PBS, *APPENDIX 2A*)

Fixative: 4% (w/v) paraformaldehyde in PBS (see recipe) or ice-cold methanol

0.1% Triton X-100 in PBS

10% fetal bovine serum (FBS) in PBS

Primary antibody:

- Rabbit anti-Atg16L1 (Cosmo Bio, catalog no. CAC-TMD-PH-AT16L, or MBL International, catalog no. PM040, both at 1:100 dilution)
- Rabbit anti-Atg12 (Cell Signaling, catalog no. 2010, 1:200 dilution)
- Mouse anti-LC3 (NanoTools, 1:1000 dilution)

Secondary antibody: e.g., goat anti-rabbit or anti-mouse conjugated to Alexa Fluor 488 or 594 (Invitrogen)

ProLong Gold antifade reagent with DAPI (Invitrogen)

13 × 13−mm coverslips

6-well culture plates

Cellomics ArrayScan VTI HCS Reader (ThermoScientific) *or* LSM 710 confocal microscope (Zeiss) and ImageJ software

Prepare cells for imaging

1. Place a 13 × 13−mm square coverslip in each well of a 6-well plate and then seed the wells with 1–2 × 10^5 cells. Culture cells overnight.

   The confluency of the cells is critical at this stage. Too high a density will preclude automatic counting of vesicles, since the microscope will be not able to focus properly on the cells.

2. *Optional (for transiently expressed proteins):* Transfect cells the following day, e.g., with 0.5 μg GFP-Atg16L1 or GFP-LC3 expression construct using a commercial transfection reagent according to the manufacturer's protocol. Culture transfected cells overnight (e.g., 16-24 hr).

3. The day after transfection or seeding, replace medium with 1-2 ml HBSS to stimulate autophagy by amino acid and serum starvation. Incubate 1-4 hr under normal culture conditions.

   This greatly facilitates the analysis, since it induces the production of autophagic precursors, facilitating their detection by microscopy (Ravikumar et al., 2010a). Do not wash cells prior to addition of HBSS, as this subjects cells to very harsh starvation conditions and may reduce cell survival.

4. Fix cells for 5 min with 4% paraformaldehyde at room temperature or with ice-cold methanol (if staining for endogenous LC3).

   Be careful not to overfix the cells. Paraformaldehyde fixation for >5 min will increase the GFP background signal, which will interfere with detection of vesicles. When immunostaining for LC3, methanol fixation gives decreased background and increased staining compared to paraformaldehyde fixation.

5. Wash cells three times with 1-2 ml PBS at room temperature.

   Cells are ready for immunostaining of endogenous proteins (steps 6-10) or direct microscopic analysis of exogenous tagged proteins (proceed to step 11).

Perform immunostaining (optional)

6. Permeabilize cells with 1-2 ml 0.1% Triton X-100 in PBS for 5 min, wash three times with 1-2 ml PBS, and incubate cells for 30 min in 1 ml of 10% FBS in PBS.

7. Add primary antibody at the appropriate dilution in 10% FBS/PBS and incubate for 2-24 hr.

   The antibody concentration and incubation conditions will vary depending on the antibody and must be determined by the user. In order to reduce the amount of antibody used, coverslips can be removed from the plate and placed onto Parafilm in a humidified chamber (e.g., a plastic box with damp tissue). Coverslips can be placed cell-side up and covered with ∼200 μl incubation buffer, or cell-side down onto 50 μl of incubation buffer. Carry out antibody incubations at room temperature for shorter times or at 4°C for longer times.

8. Wash three times with 1-2 ml PBS.

9. Add secondary antibody at 1:500 and incubate for 30 min as described for primary antibody.

   Starting at this point, avoid direct exposure of plates or slides to light, as this may result in bleaching of the signal.

10. Wash twice in 1-2 ml PBS and once in 1-2 ml water. Mount samples using ProLong Gold antifade reagent with DAPI, and keep in the dark at 4°C until microscopy analysis.

Capture images and collect data

11. On a Cellomics ArrayScan VTI HCS Reader, use the Spot Detector Bioapplication protocol (version 3) to count the number of vesicles per cell and measure the size of the vesicles (Fig. 15.16.3). Alternatively, follow these steps to manually count and measure vesicles using a confocal microscope and ImageJ software:

    a. Take high-resolution images of the cells using a confocal microscope.
    b. Open images in ImageJ.
    c. Split the channels.
    d. Invert the picture to make the background white.
    e. Adjust the threshold to remove background signal, then apply threshold.
    f. Open Analyze Particles in Analyze option, then click Apply.
    g. A table will be given showing the number of vesicles and their sizes.

BASIC PROTOCOL 3

IDENTIFICATION OF AUTOPHAGIC STRUCTURES BY ELECTRON MICROSCOPY

Electron microscopy (EM) is a useful approach to study autophagy and is particularly helpful in visualizing the localization of autophagic proteins. Immunogold labeling on ultrathin cryosections is a favorable approach to visualize autophagic structures (Tokuyasu, 1978). However, the use of this technique presents some challenges, such as the need for antibodies that work properly with aldehyde fixation and the fragility of the autophagic structures. The ultrathin cryosections are 60-nm-thick frozen sections without support (unlike Epon-embedded sections). For this reason, the sections are fragile and have a tendency to "lose" organelles that are not strongly attached to the cytoskeleton, including internal parts of double-membrane organelles. The autophagosomes (which are double-membrane organelles) are easily lost in cryosections. Over the past few years, several strategies have been used to resolve this problem, and some approaches to improve morphology and allow recognition of autophagic organelles are described below.

Recently, another modification of immunogold labeling on ultrathin cryosections was described for studying autophagy in yeast (Griffith et al., 2008), involving the use of periodic acid during fixation. This stabilized the yeast wall, allowing clarification of the early stage of autophagosome biogenesis (Mari et al., 2010).

The classical Epon embedding method is useful for autophagy research. This approach allows one to cut thicker sections that can be used for EM tomography, a useful method that gives a three-dimensional (3D) image of cell ultrastructure (Yla-Anttila et al., 2009a). EM tomography has enabled demonstration of direct connections between autophagic structures and other cellular organelles (Eskelinen et al., 2011). Epon EM does have some disadvantages. The lack of immunolabeling makes it difficult to confidently identify structures such as autophagosomes, and the high viscosity of the resin makes the method prone to artifacts.

This protocol for immunogold labeling of ultrathin cryosections is illustrated in Fig. 15.16.4. The method provides good morphology and the ability to localize autophagic markers using single or double labeling. This allows a more precise analysis of the pathways/compartments involved in the generation of an autophagosome.

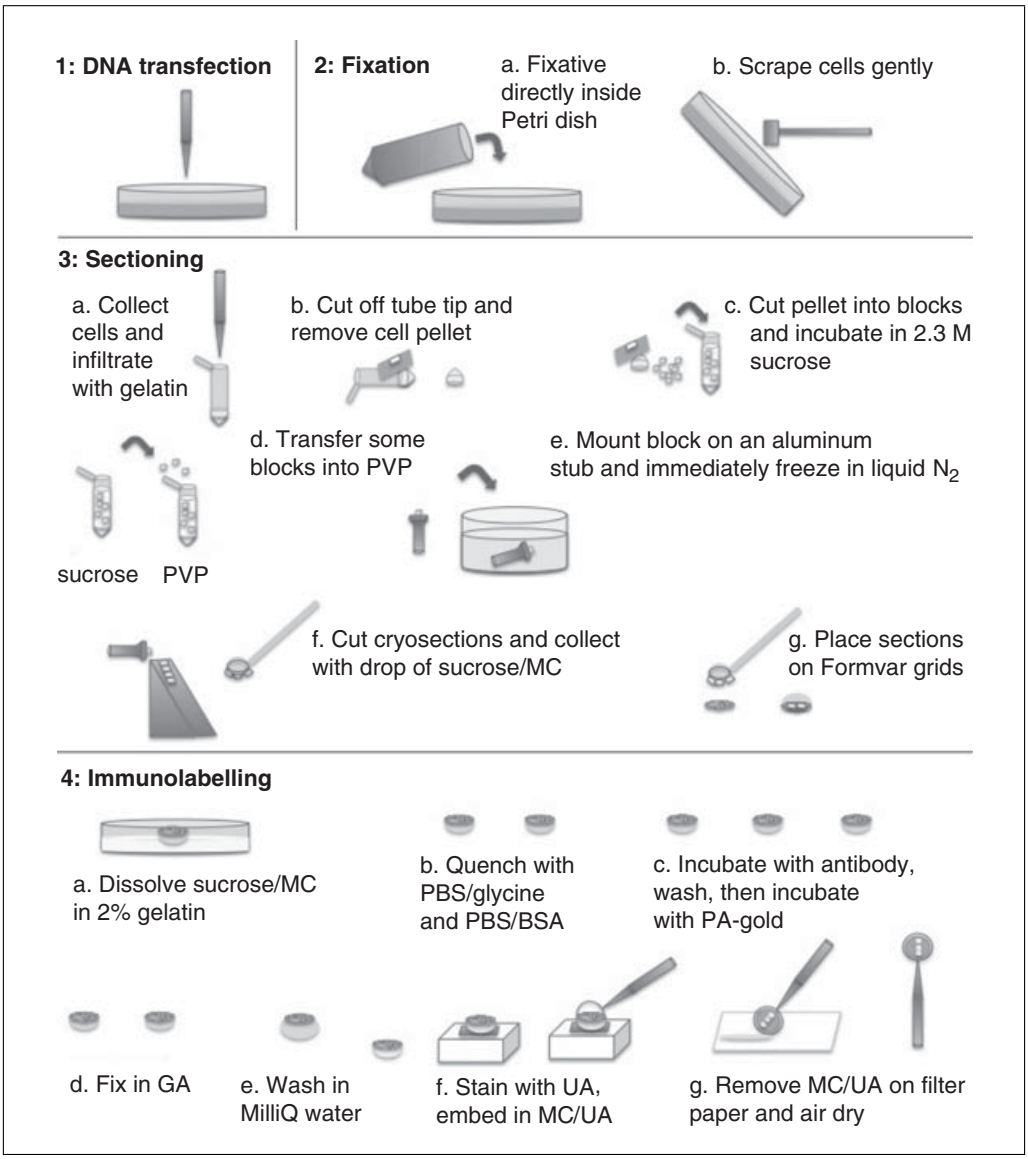

Figure 15.16.4 Schematic diagram of cell preparation for electron microscopy with immunogold labeling. Abbreviations: BSA, bovine serum albumin; GA, glutaraldehyde; MC, methylcellulose; PA-gold, protein A–gold; PVP, polyvinylpyrrolidone; UA, uranyl acetate.

Materials

HeLa cells at 70% confluency in 10-cm Petri dishes
Overexpression plasmid: e.g., GFP-Atg16L1 (Mizushima et al., 2003), FLAG-Atg16 (Cadwell et al., 2008), or GFP-LC3 (Kabeya et al., 2000)
Transfection reagent (e.g., Lipofectamine 2000, Invitrogen, or TransIT2020)
Hank's balance salt solution (HBSS, Sigma)
4% paraformaldehyde/0.4% glutaraldehyde (see recipe)
Phosphate-buffered saline (PBS, *APPENDIX 2A*)
0.2% (w/v) glycine in PBS
12% (w/v) gelatin solution (see recipe)
2.3 M sucrose solution (see recipe)
15% PVP in 1.7 M sucrose (optional, see recipe)
Liquid nitrogen
1% methylcellulose/1.15 M sucrose (see recipe)
0.1% and 1% (w/v) bovine serum albumin (BSA) in PBS

Primary antibody: anti-GFP (Invitrogen, whole serum, A-6455, 1:100), anti-FLAG (Sigma M2, 1:100), or anti-Atg16L1 (Cosmo Bio, 1:25)
Protein A−gold (CMC-Utrecht, NL)
1% (w/v) glutaraldehyde in PBS
MilliQ-purified water
2% uranyl acetate solution, pH 7.0 (see recipe)
1.8% methylcellulose/0.4% uranyl acetate (see recipe)

Cell scrapers
1.5- and 2-ml microcentrifuge tubes
Benchtop centrifuge with swinging rotor for microcentrifuge tubes
Tube rotator
Toothpicks
Cryoultramicrotome (e.g., Leica ultracut UCT with EM FCS cryochamber)
Dry diamond knife, cryo, 45°, 3 mm (Diatome or Drukker International)
200-mesh carbon-coated Formvar copper grids (Agar Scientific)
Filter paper

Prepare cells for electron microscopy

1. Transfect HeLa cells at a confluency of 70% with GFP-Atg16L1, FLAG-Atg16, or GFP-LC3 in a 10-cm Petri dish using a commercial transfection reagent according to manufacturer's instructions. Culture cells overnight.
2. Replace medium with 5-10 ml HBSS and incubate for 2 hr under normal culture conditions to induce autophagy by serum and amino acid starvation.
3. Add an equal volume of 4% paraformaldehyde/0.4% glutaraldehyde fixative to the cells (final 2% and 0.2%) and fix for 2 hr at room temperature.

   It is best to add the fixative directly to the culture medium.

Section samples

4. Rinse cells twice with 5-10 ml of 0.2% glycine/PBS and incubate at least 15 min at room temperature. In the meantime, melt a solution of 12% gelatin in PBS.
5. Place 1 ml melted gelatin into the Petri dish and scrape the cells into a 1.5-ml microcentrifuge tube as fast as possible before the gelatin solidifies.
6. Centrifuge 1 min at 13,000 rpm in a swinging rotor microcentrifuge to obtain a pellet at the bottom of the tube. Remove the gelatin, gently resuspend the pellet in fresh warm gelatin, and centrifuge again.
7. Place tube on ice for at least 15 min.
8. Cut off the tip of the tube and gently remove the cell pellet. Cut square blocks <1 mm, keeping the blocks as uniform as possible.
9. Incubate blocks overnight in 1.7 ml of 15% PVP in 2.3 M sucrose solution in a 2-ml microcentrifuge tube at 4°C on a tube rotator.

   This method has been demonstrated to improve morphology and conserve autophagosome structure (Fig. 15.16.5; Liou et al., 1996, 1997).

10. With a toothpick, remove one block from the solution, mount it on a cryoultramicrotome aluminum stub, and immediately freeze in liquid nitrogen. Store remaining blocks in PVP/sucrose at 4°C until immediately before cutting.
11. Section blocks using a cryoultramicrotome.

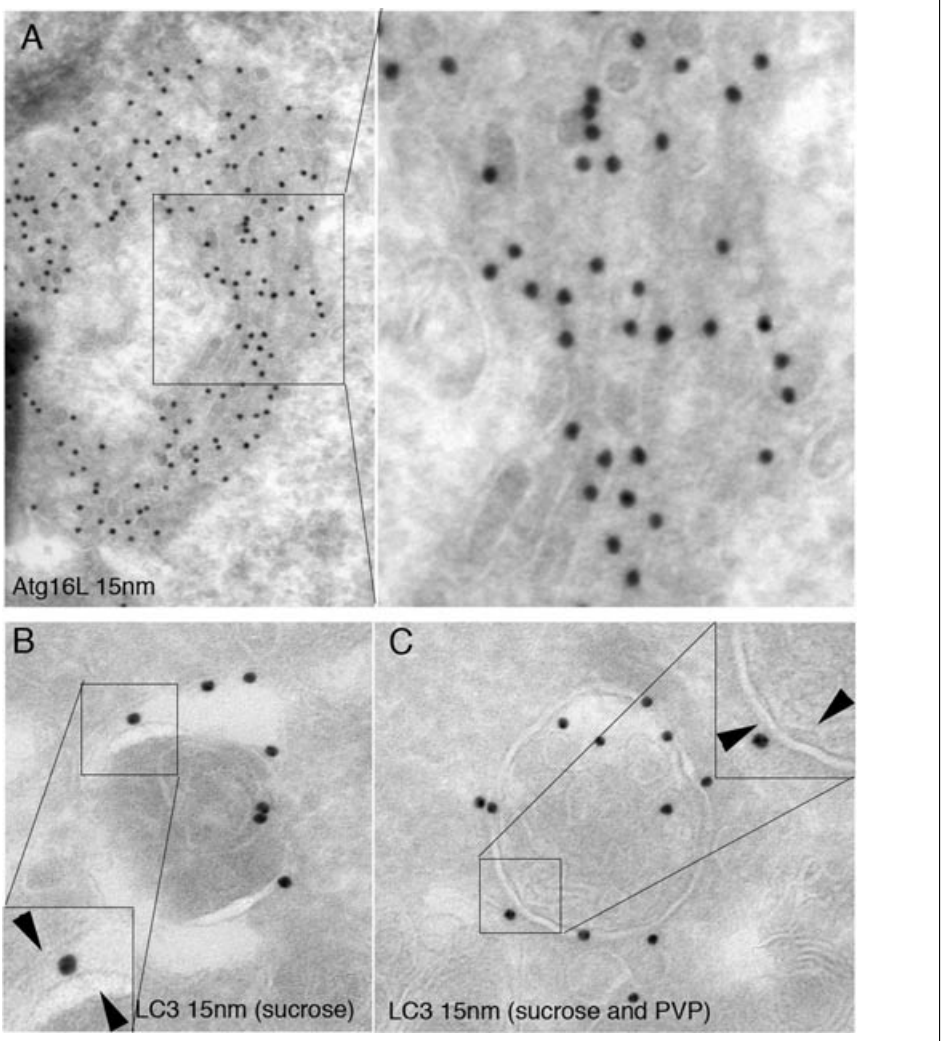

Figure 15.16.5 Representative EM images of autophagic structures. (**A**) GFP-Atg16 labeling using anti-GFP identifies pre-autophagosomal structures, which appear as tubular-vesicular structures that form clusters in the cytoplasm. (**B,C**) Morphology of autophagosomes in cells infiltrated with sucrose alone (B) or sucrose and PVP (C). The characteristic double membrane of the autophagosomes has collapsed in B but not in C. Arrows in inserts point to two membranes (white). In all images, gold particles = 15 nm.

The optimal thickness is ~75 nm (the thinner the section, the more cytoplasm and organelles are lost). It is possible to estimate section thickness by color. Sections with the correct thickness will have an intense gold color with a silky consistency when stretched. If sections are too thick, they will be brownish; if too thin, they will be silver.

12. Pick up a ribbon of sections with a drop of 1% methylcellulose/1.15 M sucrose and transfer to a 200-mesh Formvar carbon-coated copper grid.

    Sections can be stored in a cold room for several months.

Perform immunogold labeling

In all subsequent steps, treat or wash samples by placing the grids sample-side down on top of the solution for the indicated times. Do not allow samples to dry out, and keep the reverse side of the grids dry at all times.

13. Incubate grids by floating on a sequential series of solutions:

5-20 min in melted 2% gelatin in PBS at 37°C
3 × 2 min in 0.2% glycine/PBS
1-2 min in 0.1% BSA in PBS.

The melted gelatin serves to dissolve the methylcellulose/sucrose coating.

For additional details on immunogold labeling, see Goldstein and Watkins (2008).

14. Incubate the grids for 30 min in primary antibody diluted in 1% BSA/PBS.
15. Wash grids three times for 2 min in 0.1% BSA/PBS.
16. Incubate grids for 30 min in a 1:50 solution of protein A−gold in 1% BSA/PBS.
17. Rinse grids twice for 2 min in 0.1% BSA/PBS and twice for 2 min in PBS alone.
18. Fix sections for 5 min in 1% glutaraldehyde in PBS.

    This post-fixation stabilizes the interaction between the protein A−gold, antibody, and antigen, and also quenches all antibody that is free of protein A−gold.

19. Remove fixative and salts by rinsing the grids six times for 1 min each with ultrapure MilliQ-purified water.
20. Stain sections for 5-7 min at room temperature in 2% uranyl acetate solution, pH 7.0.
21. Incubate for 5 min in 1.8% methylcellulose/0.4% uranyl acetate on ice.

    This step increases contrast and provides an embedding support.

22. Remove excess methylcellulose/uranyl acetate solution from around the grid using filter paper and allow grid to air-dry completely (∼10 min).

    Prepared grids can be stored indefinitely at room temperature.

BASIC PROTOCOL 4

USE OF AGGREGATE NUMBER AS A MEASURE OF PROTEIN CLEARANCE

In addition to analyzing the levels of autophagic markers in the cell, it is also useful to assess the functional activity of autophagy. One way to do this is to assess protein clearance rates. There are a number of ways to achieve this, including measurement of long-lived protein clearance by radioactive methods (Menzies et al., 2010), measurement of clearance of specific autophagy substrates using inducible cell lines (Webb et al., 2003), and methods to tag the pool of these proteins at a given timepoint, allowing their subsequent degradation to be measured (BenYounès et al., 2011).

The steps below describe a method for assessing protein levels based on the aggregation rate of aggregate-prone proteins. This method and can be easily adapted for use in different systems, depending on the mechanism used to modulate autophagy.

When transiently transfected into cultured cells, mutant huntingtin (htt) protein, which has an expanded polyglutamine repeat region, forms aggregates. The rate of aggregation of GFP-tagged exon 1 of the htt protein has been show to correlate with protein levels in the cell (Narain et al., 1999; Arrasate et al., 2004). Counting the number of htt-exon1-transfected cells containing aggregates therefore acts as a marker for protein levels in these cells. Manipulations that increase autophagy will lead to decreased protein levels and a decrease in the number of cells containing aggregates, and manipulations that decrease autophagy will have the opposite effect. Of course, changes in protein levels can result from factors other than autophagy, such as alterations in rates of protein synthesis or other protein degradation pathways. Thus, to test the contribution of autophagy to the observed

changes in aggregation, these experiments are carried out in both autophagy-competent and -incompetent cells. This protocol describes analysis in mouse embryonic fibroblasts (MEFs) lacking *Atg5*, a gene required for normal autophagic function. This protocol can be used to assess the autophagy effects of overexpression of a gene of interest or of drug treatments.

Materials

Atg5 knockout mouse embryonic fibroblasts (MEFs) and matched wildtype control MEFs
htt-exon1-Q74-GFP expression plasmid
Drug of interest or expression plasmid for gene of interest (optional)
Transfection reagent (e.g., Lipofectamine 2000, Invitrogen, or TransIT2020)
Rapamycin (positive control)
Phosphate-buffered saline (PBS, *APPENDIX 2A*)
4% paraformaldehyde (see recipe)
70% glycerol containing 1 μg/ml DAPI

13 × 13−mm coverslips
6-well plates
Fluorescence microscope with 60× objective

1. Place a 13 × 13−mm square coverslip in each well of a 6-well plate and seed with 1–2 × 10^5 MEFs/well. Prepare three coverslips for each condition. Culture cells overnight.

   The confluency of the cells is very important for these experiments. Cells should be sufficiently dense the next day that they will not die following transfection, but sufficiently sparse that they will not overgrow before the end of the experiment. Overgrowth will make aggregate counting very hard and may also attenuate the effect of certain experimental modifications on autophagy.

2. Transfect cells with 0.5 μg/well htt-exon1-Q74-GFP using a commercial transfection reagent according to manufacturer's instructions. To measure the effect of gene overexpression on autophagy, co-transfect with 1.5 μg of the construct of interest. For drug-based studies, replace the medium 4 hr after transfection with fresh medium containing the drug of interest.

   As a positive control for aggregation assays, rapamycin can be added at a final concentration of 0.2 μM.

   Using a co-transfection ratio of 1:3 for GFP-htt construct to the construct of interest allows one to assume that cells expressing GFP-htt are also overexpressing the gene of interest.

3. Incubate cells for 48 hr under normal growth conditions.

4. Wash cells in 1-2 ml PBS and the fix for 10 min at room temperature in 1 ml of 4% paraformaldehyde.

   Cells should be protected from the light (e.g., wrapped aluminum foil) from this stage onwards.

5. Wash cells three times in 1-2 ml PBS and then mount in 70% glycerol containing 1 μg/ml DAPI (or another mountant of choice).

6. Count ~400 cells from each coverslip on a standard fluorescence microscope using a 60× objective (Fig. 15.16.6). In each field, count:

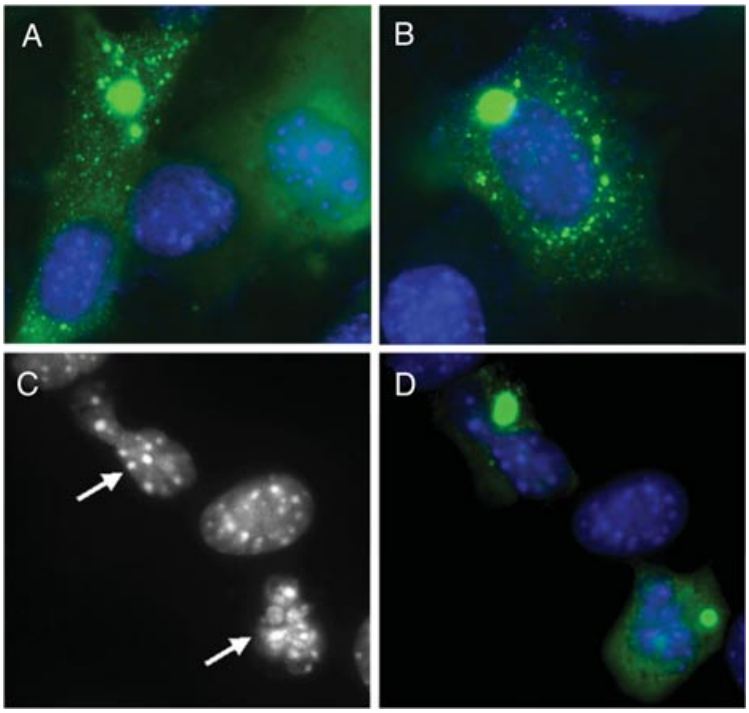

Figure 15.16.6 Aggregation in mouse embryonic fibroblasts. (**A,B**) GFP-htt Q74 aggregates in wildtype MEFs. Panel A shows a transfected cell without aggregates beside a transfected cell with aggregates. Green is GFP and blue is DAPI. (**C,D**) Abnormal nuclear morphology in MEFs transfected with HA-htt Q74. Panel C shows DAPI staining, arrows indicate cells with abnormal nuclear morphology. The same cells are shown in D, where cells with abnormal nuclei are also positive for HA-htt Q74 (green). Note that the morphology of HA aggregates is different from that of GFP aggregates, as HA aggregates sometimes have a "donut" appearance, with more intense staining around the outside of the aggregate (compare panels A, D). This is presumably due to the inability of the antibody to access the internal core of the aggregate.

a. The total number of transfected cells.
b. The number of transfected cells that contain aggregates, expressed as a percent of the total number of cells counted.
c. The number of cells with abnormal nuclei, also expressed as a percent of the total number of cells.

The identity of slides should be blinded to the observer and fields should be selected at random.

It is possible to count at higher magnification, but lower magnification can make it difficult to distinguish aggregated cells from cells with high levels of GFP fluorescence.

SUPPORT PROTOCOL

CELL CULTURE

All cell lines used in these protocols can be cultured under standard conditions.

Materials

Cells of interest:
HeLa cells, HEK cells, or MEFs
Stable cell lines, e.g., HeLa cells expressing GFP-LC3 or mRFP-GFP-LC3, HEK cells expressing GFP-DFCP1
Dulbecco's modified Eagle medium (DMEM, Sigma-Aldrich D6546)
Fetal bovine serum (FBS)

Penicillin/streptomycin solution
L-Glutamine
Phosphate-buffered saline (PBS)
1× trypsin/EDTA solution

37°C humidified 5% CO_2 incubator
75-cm^2 tissue culture flasks
Cell scrapers

Grow cells

1. Culture cells at 37°C in a humidified 5% CO_2 incubator in DMEM supplemented with:

   10% FBS
   100 U/ml penicillin/streptomycin
   2 mM L-glutamine
   500 mg/ml G418 (stable cells lines only)

   For stable cell lines expressing exogenous proteins, G418 must be added to the culture medium to ensure that the population of cells transfected with overexpression plasmid is maintained.

2. Grow cells until they reach 80%-90% confluency.

Passage cells

3. Remove medium and rinse cells once with 5-10 ml PBS.
4. Add 2.5 ml of 1× trypsin/EDTA solution to cover the cell layer. Incubate at 37°C for 3-5 min or until the cells are dissociated from the flask (no longer than 10-15 min).
5. Quench enzyme activity by adding 8 ml fresh supplemented medium and dissociate the cells by pipetting the medium up and down several times.

   Cells tend to form clumps, so it is important to dissociate clumps to give a fine suspension before re-seeding.

6. Split cells 1:5 or 1:10, re-seed in fresh supplemented medium, and return to the incubator.

REAGENTS AND SOLUTIONS

Use deionized, distilled water in all recipes and protocol steps. For common stock solutions, see ***APPENDIX 2A****; for suppliers, see* ***SUPPLIERS APPENDIX****.*

Bafilomycin A_1

Dissolve bafilomycin A_1 in DMSO to make a 100 mM stock solution. Dispense into 0.5-ml aliquots and store for up to 6 months at −20°C.

Bafilomycin A_1 is available from many suppliers (e.g., Enzo Scientific).

Gelatin solution, 12% (w/v)

Add 12 g gelatin to 100 ml PBS (*APPENDIX 2A*). Heat gently over water (~80°C), stirring continuously until dissolved. Add 200 µl of 10% (w/v) sodium azide. Store up to 6 months at 4°C.

It is best to use food-grade gelatin, which is more pure than laboratory-grade gelatin.

Lysis buffer

For 2× lysis buffer:
20 mM Tris-Cl, pH 6.8 (*APPENDIX 2A*)
137 mM NaCl
1 mM EGTA
1% Triton X-100
10% glycerol
Store up to 6 months at 4°C

For 1× lysis buffer: Dilute 2× buffer with distilled water and add protease inhibitor (Roche). Prepare fresh just before use.

Methylcellulose solution, 2% (w/v)

Heat 196 ml ultrapure distilled water to 90°C. Remove from heat and add 4 g methylcellulose (25 centipoise). Mix well, then place in an ice bucket, stirring slowly. Cover with a plastic Petri dish and leave until the solution reaches 10°C. Seal with Parafilm and leave stirring slowly overnight in a cold room. Turn off the stirrer and leave to mature for several days (at least 4 days). Collect the supernatant, leaving behind the debris that precipitates.

Methylcellulose/sucrose, 1% (w/v)/1.15 M

500 µl 2% methylcellulose solution (see recipe)
500 µl 2.3 M sucrose solution (see below)
Mix carefully, avoiding bubbles
Prepare immediately before use and keep on ice

Methylcellulose/uranyl acetate, 1.8%/0.4% (w/v)

1 volume 4% (w/v) uranyl acetate in ultrapure distilled water
9 volumes 2% methylcellulose solution (see recipe)
Prepare fresh

It is vital to prepare this solution in clean glassware, as traces of phosphate will cause the uranyl acetate to precipitate.

Paraformaldehyde, 4% (w/v)

To 4 g paraformaldehyde, add 10 ml of 10× PBS (*APPENDIX 2A*) and 70 ml distilled water. Heat to 80°C, stirring continually. If paraformaldehyde does not dissolve, add 1 N NaOH dropwise until the solution just begins to clear. Allow to cool, then check that pH is ~7.5 using pH indicator paper. Add distilled water to a total volume of 100 ml. Prepare fresh for electron microscopy. Store up to 6 months at −20°C for immunofluorescence.

Paraformaldehyde/glutaraldehyde, 4%/0.4% (w/v)

5 ml of 8% (w/v) paraformaldehyde in water
0.5 ml of 8% (w/v) glutaraldehyde in water
1 ml of 10× PBS
3.5 ml ultrapure distilled water

Polyvinylpyrrolidone (PVP)/sucrose, 15% (w/v)/1.7 M

For 20 ml, add 3 g PVP (MW 10,000) and 0.6 ml of 1.1 M Na_2CO_3 to a 50-ml Falcon tube with a magnetic stirrer and mix to create a paste. Dilute 2.3 M sucrose solution (see recipe) to 2 M with PBS and add 17 ml to the paste. Place on a flatbed shaker for several hours.

Running/transfer buffer, 10×

250 mM Tris base
1.92 M glycine
Store up to 6 months at room temperature

For 1× running buffer: Dilute 100 ml of 10× buffer with 890 ml distilled water and 10 ml of 10% (w/v) SDS (*APPENDIX 2A*). Prepare fresh.

For 1× transfer buffer: Dilute 100 ml of 10× buffer with 200 ml methanol and 700 ml distilled water. Prepare fresh.

Sample loading buffer (Laemmli buffer), 3×

187.5 mM Tris-Cl, pH 6.8 (*APPENDIX 2A*)
6% (w/v) SDS (*APPENDIX 2A*)
30% glycerol
15% β-mercaptoethanol
0.03% (w/v) bromphenol blue
Store up to 6 months at −20°C

SDS polyacrylamide gel, 12%

For 20 ml of 12% resolving gel:
8 ml 30% (37.5:1) acrylamide/bis-acrylamide solution
5 ml 1.5 M Tris-Cl, pH 8.8 (*APPENDIX 2A*)
200 µl 10% (w/v) SDS (*APPENDIX 2A*)
200 µl 10% (w/v) ammonium persulfate (APS)
8 µl *N*,*N*,*N*,*N*-tetramethylethylenediamine (TEMED)
6.6 ml distilled water

For 5 ml of 5% stacking gel:
3.4 ml 30% (37.5:1) acrylamide/bis-acrylamide solution
0.63 ml 1 M Tris-Cl, pH 6.8 (*APPENDIX 2A*)
50 µl 10% (w/v) SDS (*APPENDIX 2A*)
50 µl 10% (w/v) APS
5 µl TEMED
3.4 ml distilled water

For complete details on preparing gels, see UNIT 6.1.

Sucrose solution, 2.3 M

Add PBS to 78.7 g sucrose to a final volume of 100 ml. Heat gently above water (~80°C), stirring continuously, until dissolved.

Uranyl acetate, 2% (w/v), pH 7.0

Prepare separate solutions of 0.3 M oxalic acid and 4% (w/v) uranyl acetate, then mix 1:1. Add 25% (w/v) NH_4OH dropwise until the pH reaches 7.0. Wait for the solution to clear after each drop is added.

If the pH rises above 8, the solution will precipitate and cannot be used.

COMMENTARY

Background Information

The field of autophagy research is evolving quickly. However, there is currently no single autophagy assay that can be described as the gold standard. Depending on the system in which the process is being studied and the question being asked, different assays will be the more or less suitable.

This unit does not represent a comprehensive guide to all assays available for the study of autophagy; rather, it describes methods that we use routinely in the lab, because we find them to be the most reliable, convenient, and adaptable for use in mammalian cells. It is vital to state that none of these assays can stand alone to determine cellular autophagic activity. In order to understand the effects of a particular manipulation on autophagy, it is absolutely necessary to carry out multiple assays and compare the results of these investigations as a whole.

Immunoblotting analysis of autophagy markers

Perhaps the most experimentally straightforward method for assessing autophagy is immunoblotting for LC3-II levels. However, the interpretation of the data makes this assay more complex. Without the use of bafilomycin A_1 or a similar blocker of autophagosome degradation, it can be impossible to interpret the results. In the published literature, it is not uncommon to report LC3-II levels as a function of LC3-I. However, it has been suggested by several autophagy experts in guidelines for autophagy assays that this relative analysis is not ideal for a number of reasons: (1) some LC3-II can be delipidated and converted back to LC3-I, (2) LC3-II detection is more sensitive than LC3-I detection using immunoblotting, and (3) LC3-I levels may vary between tissues and cell lines as a result of transcriptional/translational regulation (Klionsky et al., 2008). Therefore, LC3-II levels as a function of actin or tubulin (loading control) as described here are thought to be more reliable measurements for immunoblots (Mizushima and Yoshimori, 2007; Klionsky et al., 2008).

One potential concern with the use of traditional immunoblotting for analysis of LC3-II levels is the nonlinearity of enhanced chemiluminescence (ECL). For this reason it is vital to expose the immunoblots to film for a range of exposure periods to obtain a result that is within the linear range of the ECL. As a guideline, it is suggested that one be able to read type through the band on the film; if this is not possible, the exposure time is too long. Because of this, it is often difficult to compare bands relative to LC3-II levels in the presence and absence of bafilomycin A_1 on the same film. One further way in which this issue may be addressed is by using fluorescent-based detection systems, such as IRdye infrared secondary antibodies (LI-COR), which allow greater linear ranges than ECL. These secondary antibodies are used in place of HRP-conjugated secondary antibodies, following the same protocol as described above, and are then visualized using an Odyssey scanner (LI-COR).

Notably, the analysis of synthesis rates in the presence of bafilomycin A_1 does not require that the autophagy system be at steady state. This is useful for many studies with autophagy-modulating drugs, where it may be difficult to know if they have identical effects on autophagic flux at all times after application (Sarkar et al., 2009). This makes it possible to test the effects of a drug on autophagosome synthesis at various times after starting the drug treatment.

Microscopy-based marker analysis

Monitoring the number of autophagosomes and autophagic precursors by microscopy-based systems is a good complement to other methods. Microscopy, especially with automatic microscopes, allows one to measure not only the number of vesicles per cell, but also their size and intensity in thousands of cells, giving more opportunity to understand a particular phenotype when you want to study the role of a protein in autophagy (for example, see Moreau et al., 2011). The main disadvantage of the study of autophagic precursors is that, while an increase in precursor formation can be observed, no information can be established as to whether these precursors go on to form fully functional autophagosomes that fuse with lysosomes and result in increased autophagic activity in the cell.

Electron microscopy of autophagy structures

The first studies of autophagy were carried out by electron microscopy. For the most part, studies of the ultrastructure of autophagy have been performed using the classical Epon embedding approach, which also gives the opportunity for EM tomography. However, the strong fixatives (e.g., osmium tetroxide), the viscosity of the embedding resin, and the solvents make this technique prone to artifacts (Eskelinen et al., 2011). Here we describe immunogold labeling of cryosections as an alternative technique that allows one to combine localization of autophagic marker proteins with ultrastructural analysis. This technique can also give artifacts due to the fragility of the autophagosomes. In fact, one frequently loses the internal membrane and all the organelles inside the mature autophagosomes. The use of PVP can help to preserve more of the autophagosome structure. It is important to note

that immunolabeling is sometimes weak with EM, because the analysis is performed not on the entire cell thickness, but in a section that is only nanometers thick. Moreover EM analysis (for the small size of the sections) is frequently done on only 20 to 30 cells. Thus, EM analysis is often more qualitative than quantitative.

Substrate clearance

Measurement of autophagy substrate clearance is a more quantitative way to assess autophagic activity. These methods also have their own limitations, such as possible changes in protein levels due to synthesis/degradation pathways that do not relate to autophagy. The protocol described here is one of many substrate clearance methods. Historically, clearance of radioactively labeled long-lived proteins has been used to investigate autophagic flux. The protein aggregation assay suggested here is experimentally much simpler and is more sensitive to small changes in autophagic activity. Carrying out the aggregation assay in both wildtype and autophagy-incompetent cells allows one to more directly assess the contribution of autophagy to any changes in aggregation rate, and addresses the contribution of protein synthesis or other protein degradation pathways to changes in aggregate levels. The effect of changes in protein synthesis can also be addressed by measuring clearance of autophagy substrates in cell lines in which the expression of an autophagy substrate can be switched off. For example, inducible cell lines in which the expression of mutant α-synuclein induced by the addition of an antibiotic and switched off by its removal. The levels of this soluble protein can then be measured by immunoblotting (Webb et al., 2003).

Critical Parameters and Troubleshooting

Bafilomycin A_1

The importance of a saturating concentration of bafilomycin A_1 can be illustrated by experimental conditions that either block autophagosome-lysosome fusion or reduce the degradative activity of the lysosomal compartment, which would cause increased LC3-II levels in the absence of bafilomycin A_1, but no change in LC3-II levels compared to the vehicle in the presence of bafilomycin A_1. On the other hand, nonsaturating doses of bafilomycin A_1 or insufficient treatment times could result in additive effects on LC3-II levels when testing an autophagosome-lysosome fusion blocker, which could incorrectly be interpreted as an increase in autophagosome synthesis.

An additional reason why one should use bafilomycin A_1 for reasonable periods (e.g., 4 hr) is that some LC3-II on the cytosolic surface of autolysosomes converts back to LC3-I, so the reaction is to some extent reversible. As bafilomycin A_1 appears to act first by preventing degradation of lysosomal substrates (including intra-autolysosomal LC3-II), affecting autophagosome-lysosome fusion only at later time points (Yamamoto et al., 1998; Fass et al., 2006), this can potentially confound analyses using bafilomycin A_1 at short time points, if this drug does not impede the conversion of LC3-II to LC3-I at such early time points (and if this pool of LC3-II is significant). Conversely, one should also be careful not to use lysosomal inhibitors for too long, as long-term autophagy blockade will start to mediate nonspecific effects (Korolchuk et al., 2009).

Electron microscopy of autophagic structures

As mentioned earlier, the identification of mature autophagosomes is more difficult because they are easily lost in cryosections. Under the electron microscope, mature autophagosomes appear as double-membrane organelles labeled with LC3 (Figs. 15.16.5B,C). LC3 labeling appears on both the internal and external membranes. Sometimes organelles or cytoplasmic structures such as mitochondria or vesicles can be easily identified within autophagosomes (Fig. 15.16.5C). It is not always possible to clearly visualize the double membrane due to the orientation of the plane of cutting. In such cases LC3 labeling is the only way to allow recognition of an autophagosome.

Immunogold labeling

In our experience, it is possible to use a commercial antibody to Atg16L1 (Cosmo Bio) to visualize endogenous Atg16L1 in HeLa cells, but the amount of protein is sometimes insufficient for proper analysis. In such cases, it is useful to transfect cells with a tagged Atg16 and visualize the protein using an antibody against either the tag or Atg16L1.

We have not found a good antibody to LC3 that is able to recognize the endogenous protein, and thus transfection of tagged protein is the only approach available.

Protein A−gold is able to recognize just the Fc region of the primary antibody and not the Fab region, while IgG (as in the case of IgG-gold) will recognize both the primary antibody

as well as other secondary antibodies bound to the primary antibody, resulting in clustering and signal amplification. Thus, the ratio of epitope-antibody to gold is 1:1 for protein A−gold, and gives a more precise view of the antigen present in the sample. The 1:1 ratio of gold dots to antigen also provides an opportunity to perform morphometric analyses, for instance, quantifying the amount of labeling per compartment (quantified as number of gold dots per area of organelle; Moreau et al., 2011; Ravikumar et al., 2010a). The disadvantage of this approach is that protein A−gold labeling is sometimes not very strong (because it is not amplified, as is IgG gold).

Anticipated Results

Immunoblotting analysis

It is important to consider the changes in LC3-II levels in the absence and presence of bafilomycin A_1. If a compound/gene increases LC3-II levels in the absence of bafilomycin A_1, but there is no further increase in the presence of bafilomycin A_1, then there is likely a block in LC3-II degradation, which could be due to a defect in transport to the lysosome or degradation within the lysosome (Fig. 15.16.2B, outcome 1). Conversely, a drug treatment might exert a reduction in LC3-II levels in the absence or presence of bafilomycin A_1, suggesting reduced autophagosome formation (outcome 2). Less frequently, a compound/gene can cause a decrease (or no obvious change) in LC3-II in the absence of bafilomycin A_1, but a concomitant increase in the presence of bafilomycin A_1, suggesting that there is increased delivery of substrates to the lysosome and increased autophagosome synthesis (outcome 3). The most common scenario with an autophagy inducer turns out to be increased LC3-II in the presence and absence of bafilomycin A_1 (outcome 4). This situation typically occurs alongside increased delivery of autophagic substrate to lysosomes (Sarkar et al., 2007a,b; Williams et al., 2008), but can also occur if there is increased LC3-II synthesis simultaneously with decreased degradation (Renna et al., 2011).

If LC3-II levels increase in cells treated with bafilomycin A_1 and a specific chemical being tested, compared to cells treated with bafilomycin A_1 alone, then this suggests that the rate of LC3-II (autophagosome) formation has been increased by the chemical treatment, and the converse applies if LC3-II levels are decreased (Fig. 15.16.2B) (Sarkar et al., 2007b). In this context, any small effect exerted by a putative autophagy-modulating gene/drug treatment in the absence of lysosomal clamping, will be amplified by the bafilomycin A_1 treatment. The amount of LC3-II produced over 4 hr under control conditions (equivalent to the increase caused by bafilomycin A_1) is normally many-fold higher than the levels seen in the presence of autophagy enhancers (in the absence of bafilomycin A_1), as the latter is a function of both production and degradation, and enhancers of autophagosome synthesis can only result in increased flux if they also increase degradation.

Number of autophagic precursors

A stimulation of autophagy often leads to an increase in the number of Atg12, Atg16L1, DFCP1, WIPI, and LC3 vesicles per cell without significantly affecting their size (Table 15.16.1). An inhibition of autophagy can be due to inhibition of precursor formation

Table 15.16.1 Expected Changes in Vesicle Number and Size with Induction or Inhibition of Autophagy

	Autophagy induction		Autophagy inhibition	
Protein	Number	Size	Number	Size
Atg12	Up	No change	Up or down	No change or down
Atg16L1	Up	No change	Up or down	No change or down
DFCP1	Up	ND[a]	Down	ND
WIPI	Up	ND	Down	ND
LC3	Up	No change	Up or down	No change or down

[a]ND, not determined.

Table 15.16.2 Expected Results for mRFP-GFP-LC3 Staining During Autophagy Induction and Inhibition

Signal	Induction	Inhibition (formation)	Inhibition (degradation)
Red (mRFP)	Up	Down	No change or down
Yellow (mRFP+GFP)	Up	Down	Up

or maturation. In the case of a defect in formation, the number of Atg12, Atg16L1, DFCP1, WIPI, and LC3 vesicles per cell decreases. In the case of a defect in precursor maturation, the number of Atg12 and Atg16L1 vesicles per cell increases, whereas their size frequently decreases. In case of a defect in autophagosome maturation, the number of LC3 vesicles per cell increases and their size increases (Moreau et al., 2011).

Monitoring of autophagic flux using a mRFP-GFP-LC3 stable cell line

Stimulation of autophagy leads to an increase in the number of red (autolysosome) and yellow (autophagosome) vesicles per cell (Table 15.16.2). An inhibition of autophagy due to a defect in autophagosome formation leads to a decrease in red and yellow vesicles per cell. An inhibition of autophagy due to a defect in autophagosome degradation leads to an increase in the number of yellow vesicles per cell but a decrease in the number of red vesicles per cell.

Electron microscopy of autophagic structures

The pre-autophagosomes appear on the EM as a cluster of multivesicular-tubular structures that are Atg16L1-positive (Fig. 15.16.5A). The number of vesicles and the ratio of vesicles/tubules depends on the state of maturation of the pre-autophagosomal structures. First the vesicles form clusters, then they start to fuse with each other to form tubular structures (Moreau et al., 2011).

EM analysis (in cryosections as well as Epon sections) allows quantification of the number of organelles (autophagosomes or pre-autophagosomes) per cell area and/or the amount of labeling per organelle. To determine these parameters, it is normal to use the point-hit method (Yla-Anttila et al., 2009b) or software such as Image Analysis (Olympus; Ravikumar et al., 2010a; Moreau et al., 2011).

Aggregate counting in cell culture

In cells in which autophagy is compromised, an increase in the percentage of cells containing aggregates would be expected relative to control conditions, and the converse would be expected in cells with an upregulation of the autophagic process. In many cases, this is a very simple read-out. However, it is also important to assess the number of cells with abnormal nuclei. This gives a measure of cell viability, which is important because changes in cell survival may confound measurements of protein aggregation. For example, manipulations that greatly increase htt aggregation may also lead to an increase in htt toxicity and therefore an increase in cell death. If cells with aggregates die selectively, a decrease in the percentage of cells with aggregates could be seen at certain time points. Unless cell viability is also assessed, this would suggest an increase in protein clearance. As another example, if an experimental condition results in protection against cell death but not a change in protein clearance, it is possible that cells with high levels of mutant htt will be protected, resulting in an apparent increase in aggregation along with a decrease in cell viability. Counting the number of transfected cells with abnormal nuclei is a sensitive way to assess low levels of cellular toxicity.

Time Considerations

The timeline for these assays is highly dependent on the process under investigation. For example, drugs may only need to be added to cells for hours or even minutes, whereas siRNA gene knockdown experiments may take several days to achieve the full effect.

Once the cells have been treated in the desired way for immunoblot analysis of LC3-II levels, preparation of samples takes 2-4 hr. The gels can then be run and transferred the same day, and placed into primary antibody overnight, so that immunoblotting can be finished and membranes exposed to film on the second day. The timeline is similar when immunostaining cells for microscopy or aggregate counting. For these methods, the time taken to collect data will depend on the method. Automated cell counting can produce data within 1 day, whereas manual counting can be time consuming and may take much longer.

For electron microscopy, cell preparation takes at least 2 full days. It is necessary to have all solutions prepared in advance, as many of them require somewhat lengthy preparation procedures (e.g., several days in the case of methylcellulose). However, these solutions are all stable for many months at 4°C.

Literature Cited

Arrasate, M., Mitra, S., Schweitzer, E.S., Segal, M.R., and Finkbeiner, S. 2004. Inclusion body formation reduces levels of mutant huntingtin and the risk of neuronal death. *Nature* 431:805-810.

Axe, E.L., Walker, S.A., Manifava, M., Chandra, P., Roderick, H.L., Habermann, A., Griffiths, G., and Ktistakis, N.T. 2008. Autophagosome formation from membrane compartments enriched in phosphatidylinositol 3-phosphate and dynamically connected to the endoplasmic reticulum. *J. Cell Biol.* 182:685-701.

Bampton, E.T., Goemans, C.G., Niranjan, D., Muzishima, N., and Tolkovsky, A.M. 2005. The dynamics of autophagy visualized in live cells: From autophagosome formation to fusion with endo/lysosomes. *Autophagy* 1:23-36.

BenYounès, A., Tajeddine, N., Tailler, M., Malik, S.A., Shen, S., Métivier, D., Kepp, O., Vitale, I., Maiuri, M.C., and Kroemer, G. 2011. A fluorescence-microscopic and cytofluorometric system for monitoring the turnover of the autophagic substrate p62/SQSTM1. *Autophagy* 7:883-891.

Cadwell, K., Liu, J.Y., Brown, S.L., Miyoshi, H., Loh, J., Lennerz, J.K., Kishi, C., Kc, W., Carrero, J.A., Hunt, S., Stone, C.D., Brunt, E.M., Xavier, R.J., Sleckman, B.P., Li, E., Mizushima, N., Stappenbeck, T.S., and Virgin, H.W. IV. 2008. A key role for autophagy and the autophagy gene Atg16l1 in mouse and human intestinal Paneth cells. *Nature* 456:256-263.

Eskelinen, E.L., Reggiori, F., Baba, M., Kovacs, A.L., and Seglen, P.O. 2011. Seeing is believing: The impact of electron microscopy on autophagy research. *Autophagy* 7:935-956.

Fass, E., Shvets, E., Degani, I., Hirschberg, K., and Elazar, Z. 2006. Microtubules support production of starvation-induced autophagosomes but not their targeting and fusion with lysosomes. *J. Biol. Chem.* 281:36303-36316.

Goldstein, M. and Watkins, S. 2008. Immunohistochemistry. *Curr. Protoc. Mol. Biol.* 81:14.6.1-14.6.23.

Griffith, J., Mari, M., De Maziere, A., and Reggiori, F. 2008. A cryosectioning procedure for the ultrastructural analysis and the immunogold labelling of yeast Saccharomyces cerevisiae. *Traffic* 9:1060-1072.

Kabeya, Y., Mizushima, N., Ueno, T., Yamamoto, A., Kirisako, T., Noda, T., Kominami, E., Ohsumi, Y., and Yoshimori, T. 2000. LC3, a mammalian homologue of yeast Apg8p, is localized in autophagosome membranes after processing. *EMBO J.* 19:5720-5728.

Katayama, H., Yamamoto, A., Mizushima, N., Yoshimori, T., and Miyawaki, A. 2008. GFP-like proteins stably accumulate in lysosomes. *Cell Struct. Funct.* 33:1-12.

Kimura, S., Noda, T., and Yoshimori, T. 2007. Dissection of the autophagosome maturation process by a novel reporter protein, tandem fluorescent-tagged LC3. *Autophagy* 3:452-460.

Klionsky, D.J., Abeliovich, H., Agostinis, P., et al. 2008. Guidelines for the use and interpretation of assays for monitoring autophagy in higher eukaryotes. *Autophagy* 4:151-175.

Korolchuk, V.I., Mansilla, A., Menzies, F.M., and Rubinsztein, D.C. 2009. Autophagy inhibition compromises degradation of ubiquitin-proteasome pathway substrates. *Mol. Cell* 33:517-527.

Liou, W., Geuze, H.J., and Slot, J.W. 1996. Improving structural integrity of cryosections for immunogold labeling. *Histochem. Cell Biol.* 106:41-58.

Liou, W., Geuze, H.J., Geelen, M.J., and Slot, J.W. 1997. The autophagic and endocytic pathways converge at the nascent autophagic vacuoles. *J. Cell Biol.* 136:61-70.

Mari, M., Griffith, J., Rieter, E., Krishnappa, L., Klionsky, D.J., and Reggiori, F. 2010. An Atg9-containing compartment that functions in the early steps of autophagosome biogenesis. *J. Cell Biol.* 190:1005-1022.

Menzies, F.M., Hourez, R., Imarisio, S., Raspe, M., Sadiq, O., Chandraratna, D., O'Kane, C., Rock, K.L., Reits, E., Goldberg, A.L., and Rubinsztein, D.C. 2010. Puromycin-sensitive aminopeptidase protects against aggregation-prone proteins via autophagy. *Hum. Mol. Genet.* 19:4573-4586.

Mizushima, N. and Yoshimori, T. 2007. How to interpret LC3 immunoblotting. *Autophagy* 3:542-545.

Mizushima, N., Kuma, A., Kobayashi, Y., Yamamoto, A., Matsubae, M., Takao, T., Natsume, T., Ohsumi, Y., and Yoshimori, T. 2003. Mouse Apg16L, a novel WD-repeat protein, targets to the autophagic isolation membrane with the Apg12-Apg5 conjugate. *J. Cell Sci.* 116:1679-1688.

Moreau, K., Ravikumar, B., Renna, M., Puri, C., and Rubinsztein, D.C. 2011. Autophagosome precursor maturation requires homotypic fusion. *Cell* 146:303-317.

Narain, Y., Wyttenbach, A., Rankin, J., Furlong, R.A., and Rubinsztein, D.C. 1999. A molecular investigation of true dominance in Huntington's disease. *J. Med. Genet.* 36:739-746.

Ravikumar, B., Moreau, K., Jahreiss, L., Puri, C., and Rubinsztein, D.C. 2010a. Plasma membrane contributes to the formation of pre-autophagosomal structures. *Nat. Cell Biol.* 12:747-757.

Ravikumar, B., Sarkar, S., Davies, J.E., Futter, M., Garcia-Arencibia, M., Green-Thompson, Z.W., Jimenez-Sanchez, M., Korolchuk, V.I., Lichtenberg, M., Luo, S., Massey, D.C., Menzies, F.M., Moreau, K., Narayanan, U., Renna, M., Siddiqi, F.H., Underwood, B.R., Winslow, A.R., and Rubinsztein, D.C. 2010b. Regulation of mammalian autophagy in physiology and pathophysiology. *Physiol. Rev.* 90:1383-1435.

Renna, M., Schaffner, C., Winslow, A.R., Menzies, F.M., Peden, A.A., Floto, R.A., and Rubinsztein, D.C. 2011. Autophagic substrate clearance requires activity of the syntaxin-5 SNARE complex. *J. Cell Sci.* 124:469-482.

Sarkar, S., Davies, J.E., Huang, Z., Tunnacliffe, A., and Rubinsztein, D.C. 2007a. Trehalose, a novel mTOR-independent autophagy enhancer, accelerates the clearance of mutant huntingtin and alpha-synuclein. *J. Biol. Chem.* 282:5641-5652.

Sarkar, S., Perlstein, E.O., Imarisio, S., Pineau, S., Cordenier, A., Maglathlin, R.L., Webster, J.A., Lewis, T.A., O'Kane, C.J., Schreiber, S.L., and Rubinsztein, D.C. 2007b. Small molecules enhance autophagy and reduce toxicity in Huntington's disease models. *Nat. Chem. Biol.* 3:331-338.

Sarkar, S., Korolchuk, V., Renna, M., Winslow, A., and Rubinsztein, D.C. 2009. Methodological considerations for assessing autophagy modulators: A study with calcium phosphate precipitates. *Autophagy* 5:307-313.

Sarkar, S., Korolchuk, V.I., Renna, M., Imarisio, S., Fleming, A., Williams, A., Garcia-Arencibia, M., Rose, C., Luo, S., Underwood, B.R., Kroemer, G., O'Kane, C.J., and Rubinsztein, D.C. 2011. Complex inhibitory effects of nitric oxide on autophagy. *Mol. Cell* 43:19-32.

Seglen, P.O. and Reith, A. 1976. Ammonia inhibition of protein degradation in isolated rat hepatocytes. Quantitative ultrastructural alterations in the lysosomal system. *Exp. Cell Res.* 100:276-280.

Tanida, I., Sou, Y.S., Ezaki, J., Minematsu-Ikeguchi, N., Ueno, T., and Kominami, E. 2004. HsAtg4B/HsApg4B/autophagin-1 cleaves the carboxyl termini of three human Atg8 homologues and delipidates microtubule-associated protein light chain 3- and GABAA receptor-associated protein-phospholipid conjugates. *J. Biol. Chem.* 279:36268-36276.

Tanida, I., Minematsu-Ikeguchi, N., Ueno, T., and Kominami, E. 2005. Lysosomal turnover, but not a cellular level, of endogenous LC3 is a marker for autophagy. *Autophagy* 1:84-91.

Tokuyasu, K.T. 1978. A study of positive staining of ultrathin frozen sections. *J. Ultrastruct. Res.* 63:287-307.

Underwood, B.R., Imarisio, S., Fleming, A., Rose, C., Krishna, G., Heard, P., Quick, M., Korolchuk, V.I., Renna, M., Sarkar, S., García-Arencibia, M., O'Kane, C.J., Murphy, M.P., and Rubinsztein, D.C. 2010. Antioxidants can inhibit basal autophagy and enhance neurodegeneration in models of polyglutamine disease. *Hum. Mol. Genet.* 19:3413-3429.

Webb, J.L., Ravikumar, B., Atkins, J., Skepper, J.N., and Rubinsztein, D.C. 2003. Alpha-Synuclein is degraded by both autophagy and the proteasome. *J. Biol. Chem.* 278:25009-25013.

Williams, A., Sarkar, S., Cuddon, P., Ttofi, E.K., Saiki, S., Siddiqi, F.H., Jahreiss, L., Fleming, A., Pask, D., Goldsmith, P., O'Kane, C.J., Floto, R.A., and Rubinsztein, D.C. 2008. Novel targets for Huntington's disease in an mTOR-independent autophagy pathway. *Nat. Chem. Biol.* 4:295-305.

Yamamoto, A., Tagawa, Y., Yoshimori, T., Moriyama, Y., Masaki, R., and Tashiro, Y. 1998. Bafilomycin A1 prevents maturation of autophagic vacuoles by inhibiting fusion between autophagosomes and lysosomes in rat hepatoma cell line, H-4-II-E cells. *Cell Struct. Funct.* 23:33-42.

Yla-Anttila, P., Vihinen, H., Jokitalo, E., and Eskelinen, E.L. 2009a. 3D tomography reveals connections between the phagophore and endoplasmic reticulum. *Autophagy* 5:1180-1185.

Yla-Anttila, P., Vihinen, H., Jokitalo, E., and Eskelinen, E.L. 2009b. Monitoring autophagy by electron microscopy in Mammalian cells. *Methods Enzymol.* 452:143-164.